

Computationally Efficient Lattice Reduction Aided Detection for MIMO-OFDM Systems under Correlated Fading Channels

Wei Liu, Kwonhue Choi, and Huaping Liu

We analyze the relationship between channel coherence bandwidth and two complexity-reduced lattice reduction aided detection (LRAD) algorithms for multiple-input multiple-output (MIMO) orthogonal frequency division multiplexing (OFDM) systems in correlated fading channels. In both the adaptive LR algorithm and the fixed interval LR algorithm, we exploit the inherent feature of unimodular transformation matrix \mathbf{P} that remains the same for the adjacent highly correlated subcarriers. Complexity simulations demonstrate that the adaptive LR algorithm could eliminate up to approximately 90 percent of the multiplications and 95 percent of the divisions of the brute-force LR algorithm with large coherence bandwidth. The results also show that the adaptive algorithm with both optimum and globally suboptimum initial interval settings could significantly reduce the LR complexity, compared with the brute-force LR and fixed interval LR algorithms, while maintaining the system performance.

Keywords: MIMO, OFDM, coherence bandwidth, lattice reduction.

Manuscript received Nov. 13, 2011; revised Dec. 28, 2011; accepted Jan. 12, 2012.

This paper was presented in part at IEEE 6th International Conference on Wireless and Mobile Computing, Networking and Communications, Niagara Falls, Canada, October 2010.

This research was supported by the Ministry of Knowledge Economy, Korea, under the Information Technology Research Center support program supervised by the National IT Industry Promotion Agency (NIPA-2012-C1090-1231-0009) and Basic Science Research Program through the National Research Foundation of Korea funded by the Ministry of Education, Science and Technology (2009-0088286).

Wei Liu (phone: +1 541 740 0192, liu@eecs.oregonstate.edu) and Huaping Liu (hliu@eecs.oregonstate.edu) are with the Department of Electrical Engineering and Computer Science, Oregon State University, Corvallis, OR, USA.

Kwonhue Choi (gonew@ynu.ac.kr) is with the Department of Information and Communication Engineering, Yeungnam University, Gyeongsan, Rep. of Korea.

<http://dx.doi.org/10.4218/etrij.12.0111.0707>

I. Introduction

Multiple-input multiple-output (MIMO) antennas combined with orthogonal frequency division multiplexing (OFDM) could potentially provide both high data rates and a high spectral efficiency in frequency-selective fading channels [1]. For MIMO signal detection, the maximum likelihood (ML) algorithm achieves optimal performance but is computationally prohibitive. On the other hand, linear detection schemes such as the zero-forcing (ZF) or minimum mean square error (MMSE) algorithms are simple, but they result in significant performance degradation. Lattice reduction aided detection (LRAD) is regarded as a suboptimal solution for detection in MIMO systems in that it realizes full diversity with some penalty in the signal-to-noise ratio (SNR) to achieve the same bit error rate (BER) as the BER of the ML scheme. An efficient but not optimal method to compute the reduced channel matrix was proposed in [2], known as the LLL algorithm. However, the computation needs for the LLL algorithm are still high, especially for systems with a large number of antennas.

A complexity-reduced LRAD technique was proposed in [3], where large reduction in complexity could be achieved by using temporal correlation of the fading channel. Another computationally efficient LR algorithm for time varying channels is proposed in [4], where it is found that the unimodular transformation matrices of LR frequently remain the same for quite a few adjacent channel matrices; in a slow fading channel, they may remain the same for several tens of consecutive channel matrices.

Both [3] and [4] focus on the correlation in the time domain.

Our previous research [5] revealed that for a MIMO-OFDM system in a channel with a large coherence bandwidth B_c , the LR unimodular transformation matrices remain the same for many adjacent subcarriers. Inspired by this observation, we proposed a reduced complexity LR algorithm [5] that significantly reduces the computational needs of lattice reduction for MIMO-OFDM detection, referred to as the adaptive LR algorithm. This algorithm fully exploits the correlation of channel matrices among successive subcarriers in the frequency domain. Besides, a fixed direct calculation interval is used in [4], which is not efficient especially when the fading rate of the time-varying channel changes. This inspires us to develop an adaptive direct calculation interval setting in the proposed algorithm.

This computationally efficient LRAD algorithm can be deployed in most MIMO-OFDM based wireless systems, such as 3GPP Long Term Evolution (LTE), IEEE 802.11n, and 802.16, since they work on frequency-selective fading channels.

The remainder of this paper is organized as follows. In section II, we briefly review the MIMO-OFDM system model and LRAD. We develop the adaptive LR algorithm and introduce the fixed interval LR algorithm in section III. The channel coherence bandwidth calculation and the initial interval setting of the adaptive LR algorithm are given in section IV. The relationship between the channel coherence bandwidth and the initial interval settings of the aforementioned algorithms is analyzed and justified by simulation results in section V. The simulation environment and comprehensive numerical results are presented in this section, as well, to corroborate our theoretical claims. Finally, section VI concludes this paper.

II. System Model and LR-Aided Detection

1. System Model

Consider an $n_t \times n_r$ MIMO system with n_t transmit and n_r receive antennas. A frequency domain narrowband model of a MIMO-OFDM system is considered as

$$\mathbf{y}(f) = \mathbf{H}(f)\mathbf{s}(f) + \mathbf{n}(f), \quad (1)$$

where $\mathbf{y} = [y_1 \ y_2 \ \dots \ y_{n_r}]^T$ (superscript \top denotes transpose), $\mathbf{s} = [s_1 \ s_2 \ \dots \ s_{n_t}]^T$, and $\mathbf{n} = [n_1 \ n_2 \ \dots \ n_{n_r}]^T$ respectively represent the received signal vector, the transmitted symbol vector, and the received noise vector. The channel matrix $\mathbf{H}(f)$ has a dimension of $n_r \times n_t$, and its m -th column, h_m , represents the channel coefficients from the m -th transmit antenna to all receive antennas. Since there is no confusion, we use \mathbf{H} instead of $\mathbf{H}(f)$ in the rest of this paper for brevity. We consider the

case in which the channel matrix \mathbf{H} is fully known at the receiver but not at the transmitter.

2. LR-Aided Detection

A lattice reduced channel matrix \mathbf{H}' can be written as

$$\mathbf{H}' = \mathbf{H}\mathbf{P}, \quad (2)$$

where \mathbf{P} is an $n_t \times n_t$ unimodular matrix with all integer elements and determinant +1 or -1. The system model for the reduced lattice can be obtained by reformulating the original system model as

$$\mathbf{y} = \mathbf{H}\mathbf{P}\mathbf{P}^{-1}\mathbf{s} + \mathbf{n} = \mathbf{H}'\mathbf{z} + \mathbf{n}, \quad (3)$$

where $\mathbf{z} = \mathbf{P}^{-1}\mathbf{s}$ is the transmitted signal in the reduced lattice. Since the reduced channel matrix is generally significantly better conditioned than the original channel matrix, LR-aided linear detection can be simply applied using the ZF or MMSE algorithms and more reliable estimates of the transmitted symbols can be obtained [6].

III. Complexity-Reduced LR-Aided Detection Algorithms

Motivated by the features of lattice reduction explained in section I, we proposed a novel complexity reduction scheme, the adaptive LR algorithm [5], based on the observation that two consecutive unimodular transformation matrices \mathbf{P}_i and \mathbf{P}_{i+1} (the subscripts are the subcarrier indices) frequently remain the same in the correlated frequency-selective channels of our interest [5]. This is because their elements are all integer valued due to a ‘‘round’’ operation in the LR algorithm and change only in the case of a substantial difference between channel matrices \mathbf{H}_i and \mathbf{H}_{i+1} . Furthermore, for the channel with a relatively large coherence bandwidth, \mathbf{P}_i may remain the same for several channel matrices of consecutive subcarriers. Moreover, to overcome the drawback of the fixed interval in [4], we make the direct calculation interval adjustable to adapt to the varying channels.

Initially, to determine if \mathbf{P}_i changes or not, we perform brute-force LR only at the two boundaries of a relatively large direct calculation interval K . Determined by the channel coherence bandwidth, K is initialized to be K_0 . We will elaborate on this issue in section IV. Note that we combine the so-called pre-multiplied LR method [7], [8] to reduce the computations for the LR operation by using pre-multiplied channel matrix $\mathbf{H}_{i+K}\mathbf{P}_i$ as the initial state of \mathbf{H}_{i+K} in the LR iterations beforehand. Then, we compare \mathbf{P}_{i+K} with \mathbf{P}_i . Depending on whether they are the same or not, either the block mode or the halve mode is enabled.

First, the block mode is actuated if \mathbf{P}_{i+K} equals \mathbf{P}_i . In this case, our conjecture is that the remaining $K-1$ \mathbf{P} matrices within this direct calculation interval are the same and equal to \mathbf{P}_i . By

setting $\mathbf{P}_j = \mathbf{P}_i$ for $i+1 \leq j \leq i+K-1$, the brute-force LR operations for a block of $K-1$ channel matrices are eliminated. Then, the corresponding lattice reduced channel matrices, \mathbf{H}'_j s, are simply obtained by performing the matrix multiplication given in (2). Therefore, this block mode reduces the total amount of calculation required for a whole LR operation into just a single matrix multiplication for each subcarrier in between.

Second, in the halve mode that is activated if \mathbf{P}_{i+K} does not equal \mathbf{P}_i , we halve the direct calculation interval; that is, the new interval is set to be $K/2$ and performs the brute-force LR operations for the new boundary $\mathbf{H}_{i+K/2}$ by using $\mathbf{H}_{i+K/2}\mathbf{P}_{i+K}$ as the initial state of $\mathbf{H}_{i+K/2}$ in the LR iterations. This comes from the expectation that $\mathbf{P}_{i+K/2}$ is more likely equal or at least similar to \mathbf{P}_{i+K} than \mathbf{P}_i is. Then, we continue to compare $\mathbf{P}_{i+K/2}$ with both previous direct calculation boundaries, that is, \mathbf{P}_i and \mathbf{P}_{i+K} . Depending on whether or not either pair is the same, another block mode or halve mode will be activated. We repeat this procedure until we obtain all the lattice reduced channel matrices \mathbf{H}'_j s for all subcarriers.

The overall procedure of the adaptive LRAD scheme is summarized in Fig. 1. For comparison, we briefly introduce the so-called fixed interval LR algorithm from [4] in Fig. 2, which can also be applied in MIMO-OFDM systems with slight modifications.

Simulation results in the next section demonstrate that the complexity reduction in the block mode, especially the block mode induced by the halve mode, is so significant that the adaptive scheme achieves greater computational efficiency than both the brute-force LR algorithm and the fixed interval LR scheme. It is worthwhile to remark that since we apply this algorithm in the frequency domain, we do not encounter the problem of buffering channel matrices of consecutive subcarriers [4], and detection latency can thus be avoided in the adaptive LR and fixed interval LR algorithms.

IV. Channel Coherence Bandwidth and Initial Interval Setting

The initial direct calculation interval setting is a key issue for both the adaptive LR algorithm and the fixed interval LR algorithm. On the one hand, if the initial calculation interval is too large, a lot more brute-force LR operations are needed due to the halve mode of the adaptive LR algorithm or the sequential mode of the fixed interval LR algorithm; on the other hand, if the initial calculation interval is too small, we may not fully utilize the channel correlation and cannot eliminate those brute-force LR operations that could be eliminated. The initial calculation interval for the adaptive LR algorithm is set according to the coherence bandwidth, which

```

1 Initialization: Set  $i=1$ ;
2 Perform LR for  $\mathbf{H}_i$ .
3 Set  $K=K_0$ , perform LR for  $\mathbf{H}_{i+K}$  with the initial setting of
    $\mathbf{H}_{i+K} = \mathbf{H}_{i+K}\mathbf{P}_i$ ;
4 if  $\mathbf{P}_{i+K} = \mathbf{P}_i$ : block mode
5   for  $j=i+1:i+K-1$ 
6     Set  $\mathbf{P}_j = \mathbf{P}_i$ ,
7     Compute  $\mathbf{H}'_j = \mathbf{H}_j\mathbf{P}_j = \mathbf{H}_j\mathbf{P}_i$ .
8   end for
9 else halve mode
10  Set  $K=K/2$ ,
11  Perform LR for  $\mathbf{H}_{i+K}$  with the initial setting of
      $\mathbf{H}_{i+K} = \mathbf{H}_{i+K}\mathbf{P}_{i+2K}$ ;
12 if  $\mathbf{P}_{i+K} = \mathbf{P}_i$ : block mode
13   for  $j=i+1:i+K-1$ 
14     Set  $\mathbf{P}_j = \mathbf{P}_i$ ,
15     Compute  $\mathbf{H}'_j = \mathbf{H}_j\mathbf{P}_j = \mathbf{H}_j\mathbf{P}_i$ .
16   end for
17 end if
18 if  $\mathbf{P}_{i+K} = \mathbf{P}_{i+2K}$ : block mode
19   for  $j=i+K+1:i+2K-1$ 
20     Set  $\mathbf{P}_j = \mathbf{P}_{i+K}$ ,
21     Compute  $\mathbf{H}'_j = \mathbf{H}_j\mathbf{P}_j = \mathbf{H}_j\mathbf{P}_{i+K}$ .
22   end for
23 else go to step 10.
24 end if
25 end if
26 Set  $i=i+K_0$  and go to step 3.

```

Fig. 1. Adaptive LRAD algorithm.

```

1 Initialization: Set  $i=1$ ;
2 Perform LR for  $\mathbf{H}_i$ .
3 Perform LR for  $\mathbf{H}_{i+K}$  with initial setting of
    $\mathbf{P}_{i+K} = \mathbf{P}_i$  in the LR iteration.
4 if  $\mathbf{P}_{i+K} = \mathbf{P}_i$ : block mode
5   for  $j=1:K-1$ 
6     Set  $\mathbf{P}_{i+j} = \mathbf{P}_i$ ,
7     Compute  $\mathbf{H}_{i+j} = \mathbf{H}_{i+j}\mathbf{P}_{i+j}$ .
8   end for
9 else sequential mode
10  for  $j=1:K-1$ 
11    Perform LR for  $\mathbf{H}_{i+j}$  with initial setting of
        $\mathbf{P}_{i+j} = \mathbf{P}_{i+j-1}$  in the iteration.
12  end for
13 end if
14 Set  $i=i+K$  and go to step 3.

```

Fig. 2. Fixed interval LRAD algorithm.

can be derived from the channel frequency correlation function.

We denote T_s as the OFDM symbol duration. The subchannel spacing Δf is determined using the orthogonality principle, that is, $T_s\Delta f = 1$ [9]. Therefore, the coherence

bandwidth in terms of number of subcarriers, B_{cn} , can be determined by $B_{\text{cn}} = B_c/\Delta f = B_{\text{cn}}T_s$.

The correlated frequency-selective Ricean fading multipath channel is generated as follows. A delay profile is assumed in the form of a tapped delay-line, characterized by a number of paths at fixed positions on a sampling grid. A wide-sense stationary and uncorrelated scattering channel model with one line-of-sight (LOS) path and L_t resolvable diffused paths is considered in this paper. The time resolution of the multipath for OFDM systems, T_r , is determined by T_s/N_c , where N_c is the number of subcarriers. Assuming that all paths arrive consecutively, the maximum delay spread of multipath channel T_m , which is approximately the reciprocal of B_c , can be simply obtained by $(L_t-1)T_r$. The multipath channel impulse response from p -th ($p = 1, 2, \dots, n_t$) transmit antenna to q -th ($q = 1, 2, \dots, n_r$) receive antenna is generated as [10]

$$h_{p,q}(t) = \alpha_{\text{LOS}}^{p,q} \delta(t - \tau_{\text{LOS}}) + \sum_{l=0}^{L_t-1} \alpha_l^{p,q} \delta(t - \tau_l). \quad (5)$$

Usually, the first tap contains the LOS ray and some non-line-of-sight (NLOS) rays (only one NLOS ray is considered in the first tap in this paper). Thus, $\tau_0 = \tau_{\text{LOS}}$. Note that τ_{LOS} in (5) can always be normalized to zero without loss of generality. The total power of the diffused multipaths is $2L_t$ and the Ricean factor of the channel is thus given by $|\alpha_{\text{LOS}}^{p,q}|^2/2L_t$. Therefore, applying the Fourier transform to (5), the channel frequency response for the n -th, $n = 0, 1, \dots, N_c - 1$, subcarrier is obtained by

$$H_{p,q}(n) = \alpha_{\text{LOS}}^{p,q} e^{-j2\pi n \Delta f \tau_{\text{LOS}}} + \sum_{l=0}^{L_t-1} \alpha_l^{p,q} e^{-j2\pi n \Delta f \tau_l}, \quad (6)$$

where α_l is an independent and identically distributed circularly symmetric complex Gaussian random variable with zero mean and variance d_l^2 , and the delay for each path τ_l is equal to lT_r .

From [10], the space-frequency correlation \mathbf{R}_{LOS} between the p_1 -th transmit antenna, q_1 -th receive antenna, n_1 -th subcarrier and the p_2 -th transmit antenna, q_2 -th receive antenna, n_2 -th subcarrier is

$$\begin{aligned} \mathbf{R}_{\text{LOS}}(p_1, q_1, n_1; p_2, q_2, n_2) &= E\{H_{p_1, q_1}(n_1) H_{p_2, q_2}^*(n_2)\} \\ &= |\alpha_{\text{LOS}}|^2 \exp[-j2\pi(p_1 - p_2)d_t \sin\theta_0 - j2\pi(q_1 - q_2)d_r \sin\phi_0] \\ &\quad \times \exp[-j2\pi \Delta f(n_1 - n_2)\tau_{\text{LOS}}] \\ &\quad + \sum_{l=0}^{L_t-1} \epsilon_l^2 \chi_l^{p_1, q_1; p_2, q_2} E\{\alpha_l^{p_1, q_1} (\alpha_l^{p_2, q_2})^*\}, \end{aligned} \quad (7)$$

where d_t and d_r are the transmit antenna spacing and receive antenna spacing, respectively, normalized to the wavelength,

θ_0 is the direction-of-departure, ϕ_0 is the direction-of-arrival, ϵ_l^2 is the average power of each tap, and $\chi_l^{p_1, q_1; p_2, q_2}$ is the spatial correlation coefficient. We will use χ_l instead of $\chi_l^{p_1, q_1; p_2, q_2}$ for brevity. The elements in the channel matrix for the same subcarrier or across subcarriers become more correlated as \mathbf{R}_{LOS} increases, and, according to the property of lattice reduction, the probability that the \mathbf{P} matrix remains the same along the subcarrier axis therefore becomes larger.

In practice, spatial elements are supposed to be more or less independent to obtain maximal spatial multiplexing or diversity gains. Therefore, we will elaborate on the correlation in the frequency domain to evaluate these two algorithms in this paper with the following simplified correlation model.

For a channel with L_t resolvable channel paths and N_c subcarriers, a foundational rule is that $B_{\text{cn}} = N_c/L_t$ [11]. We verify that for this B_{cn} , the frequency correlation function is only about 0.5 and, therefore, is far too large to be used as an initial calculation interval. Regardless of antenna correlation, the correlation \mathbf{R} between any two subcarriers on the same receive antenna is a univariate function of their frequency indices span m , given by

$$\mathbf{R}(m) = E\{H(k)H^*(k-m)\} = \sum_{l=0}^{L_t-1} d_l^2 \exp(j2\pi \frac{ml}{N_c}), \quad (8)$$

where $(\cdot)^*$ and d_l^2 denote the complex conjugate and path variance, respectively [12]. Equation (8) indicates that the frequency correlation function of subcarriers is simply the discrete Fourier transform of the channel's power delay profile (PDP). Without loss of generality, the channel powers are assumed to be normalized such that $\sum_l d_l^2 = 1$.

In this paper, we consider the uniform PDP (UPDP) Ricean fading channel and therefore, the variance for each tap is

$$d_l^2 = \begin{cases} \frac{|a_{\text{LOS}}|^2 + 2}{|a_{\text{LOS}}|^2 + 2L_t}, & l = 0, \\ \frac{2}{|a_{\text{LOS}}|^2 + 2L_t}, & l = 1, \dots, L_t - 1. \end{cases}$$

From (8), we can calculate B_{cn} s with a frequency correlation function above 0.9 for the UPDP Ricean fading channel, as listed in Table 1.

After every B_{cn} for this specific channel has been calculated, we can simply apply them to the adaptive LR algorithm by setting the initial direct calculation interval. Simulation results in section V verify that a good rule of thumb for the optimum initial interval setting of the adaptive LR algorithm is $B_{\text{cn}}(\mathbf{R} = 0.9)$ divided by the number of channel matrix elements. As for the fixed interval LR algorithm, although we cannot find a closed-form relationship between the interval setting and channel coherence bandwidth, the initial interval setting

Table 1. B_{cn} with frequency correlation function above 0.9 for UPDP Ricean fading channel.

L_t	$B_{cn} (\mathbf{R}=0.9)$
10	71
5	155
3	294
2	530

Table 2. Simulation parameters for frequency-selective channel.

FFT size	2,048
Modulation	16-QAM
Bandwidth	20 MHz
Symbol duration	66.7 μ s
Subchannel spacing	15 kHz
Cyclic prefix ratio	1/4

increases slowly and monotonically as channel coherence bandwidth gets larger, which is discussed in the next section.

V. Numerical Results and Discussions

A system similar to the 3GPP LTE is employed in the simulations. We use the simulation parameters summarized in Table 2. The Ricean factor is set to be a constant and equal to 6 dB for a 2×2 case and 12 dB for a 4×4 case for all multipath fading situations.

For the 4×4 case, we plot the computational complexities of the adaptive LR and fixed interval LR algorithms in Figs. 3 and 4. Since the number of iterations in the LR operation varies depending on the channel conditions, resulting in difficulties in deriving a compact closed-form for the complexity of the algorithms, we simply count the number of computations as the complexity whenever we meet the multiplication or division operations during the simulation and compute the average n_m and n_d , where n_m and n_d denote the average number of the required real multiplications and real divisions, respectively. These figures demonstrate that the initial interval setting is significant for both LRAD algorithms. If the optimum initial interval is not used according to the coherence bandwidth, the lowest calculation complexity will not be achieved. With various simulation settings, we can find the optimum initial setting that achieves the lowest complexity under each B_{cn} for these two algorithms. For example, for the 2×2 case, the optimum initial interval for the adaptive LR algorithm is [16 32 64 128] and for the fixed interval LR algorithm is [6 8 12 18]. The initial interval for the adaptive LR

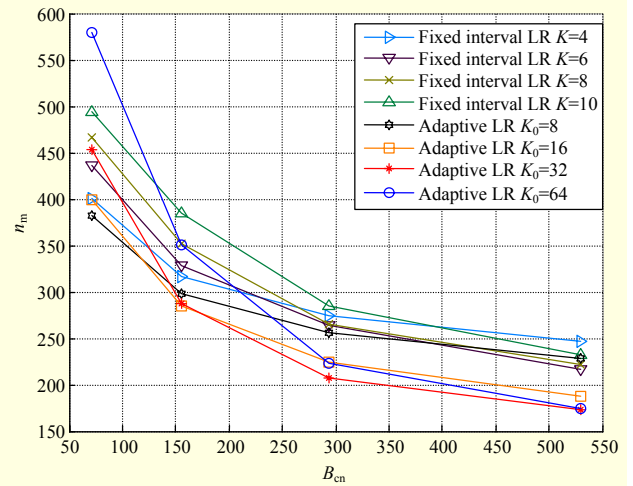


Fig. 3. Comparison of number of multiplications for various initial interval settings with two LRAD schemes for 4×4 MIMO-OFDM systems.

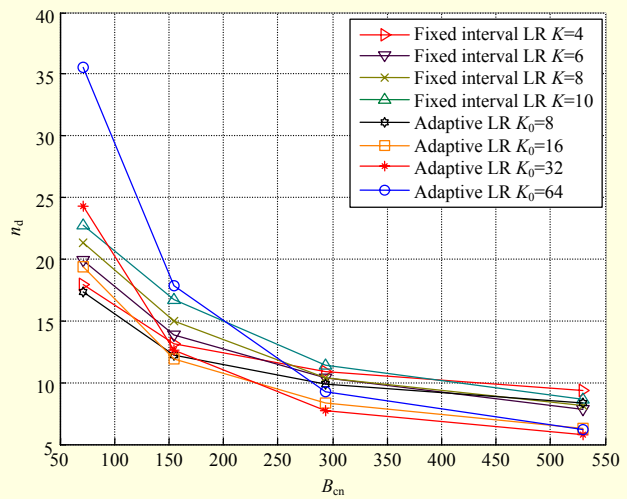


Fig. 4. Comparison of number of divisions for various initial interval settings with two LRAD schemes for 4×4 MIMO-OFDM systems.

algorithm roughly agrees with $B_{cn} = [71 \ 155 \ 294 \ 530]$ divided by 4, where 4 is the number of channel matrix elements. We also notice that, as for the adaptive LR algorithm, the initial interval setting becomes less important as the coherence bandwidth increases, which is due to the inherent adaptive property of the halve mode in this algorithm.

In Fig. 5, we plot the occurrence rate of block modes p_B and failure rate of block modes p_F under various coherence bandwidths for different configurations, where p_B is defined to indicate the probability of the reduced lattice channel matrices obtained by block modes out of the total number of channel matrices, and p_F denotes the probability that unimodular

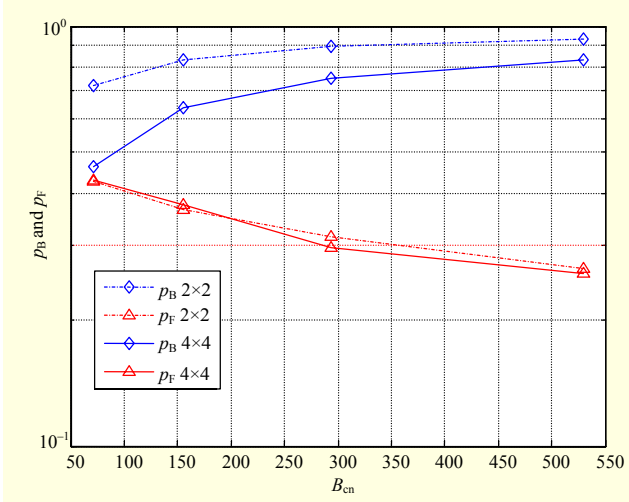


Fig. 5. Block mode occurrence rates and failure rates of adaptive LRAD for MIMO-OFDM systems with dimensions 2×2 and 4×4 .

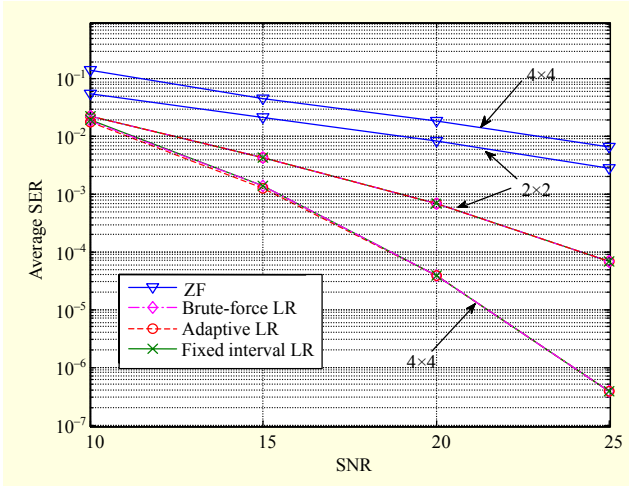


Fig. 6. SER performance of various LRAD schemes for MIMO-OFDM systems with dimensions 2×2 and 4×4 .

transformation matrices obtained in block modes are not equal to the corresponding matrices calculated by the brute-force LR algorithm, that is,

$$p_F = \Pr[\mathbf{P}_j \neq \mathbf{P}_i, \text{ for } \exists j \in [i+1, i+2, \dots, i+K-1] \mid \text{block mode}]. \quad (9)$$

With the same coherence bandwidth, as the number of antennas increases, the occurrence rate of block modes decreases. This is because as the channel matrix dimension increases, the probability that $\mathbf{P}_{i+K} = \mathbf{P}_i$ reduces. Moreover, as the coherence bandwidth increases, the failure rate of the adaptive LR scheme decreases since the channel becomes more correlated in the frequency domain. Also, even though p_F for the adaptive LR scheme is relatively high (that is, many LR results obtained by the block mode are not exactly the same as

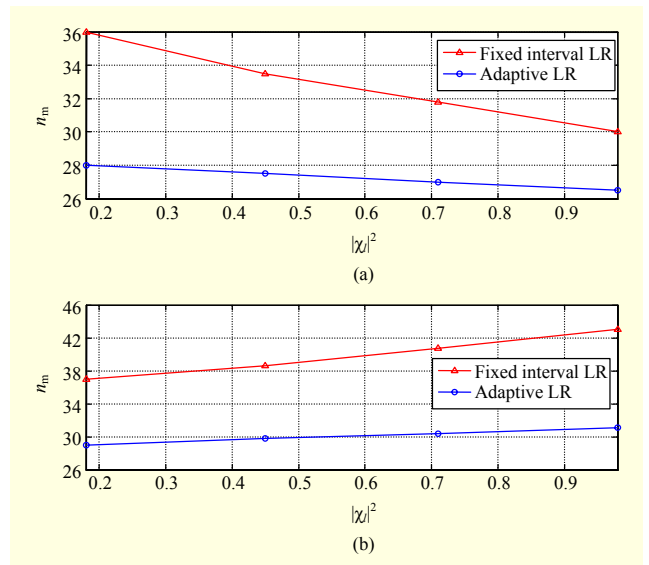


Fig. 7. Impact of spatial correlation coefficient on computational complexity for two LRAD schemes for 2×2 MIMO-OFDM systems: (a) real and imaginary parts of spatial correlation coefficient are positive; (b) real and imaginary parts of spatial correlation coefficient are negative.

the accurate results computed by the brute-force LR algorithm), the lattices obtained by the block mode are already quite reduced and orthogonalized in most cases; therefore, the performance degradation is negligible (this is justified in Fig. 6).

The symbol error rate (SER) performance of the various algorithms for MIMO-OFDM detection is compared in Fig. 6. As shown in this figure, the adaptive LR algorithm can achieve the same SER performance as the brute-force LR and fixed interval LR algorithms. The error produced by the block mode of the adaptive LR scheme is therefore insignificant and does not cause any performance degradation.

We plot the impact of the spatial correlation coefficient on the computational complexity in terms of n_m versus χ at $B_{cn} \approx 300$ in Fig. 7. From [10], χ is a complex number and the real and imaginary part of χ are uniformly distributed in the range $[0.3, 0.7]$ or $[-0.3, -0.7]$. We assume the transmit and receive antenna arrays are parallel, so the spatial correlation is independent of θ_0 and ϕ_0 . Figure 7(a) shows the results for the case in which the real and imaginary parts of χ are positive, while Fig. 7(b) corresponds to the case in which the real and imaginary parts are negative. Figure 7(a) shows that as the spatial correlation increases, the complexities of both algorithms decrease. Figure 7(b) shows that as the spatial correlation increases, the complexities of both algorithms increase, since the subcarriers have negative spatial correlations. It is worth pointing out that both figures reveal that the fixed interval LR algorithm is more sensitive to the spatial correlation; however, the impact of the spatial correlation on

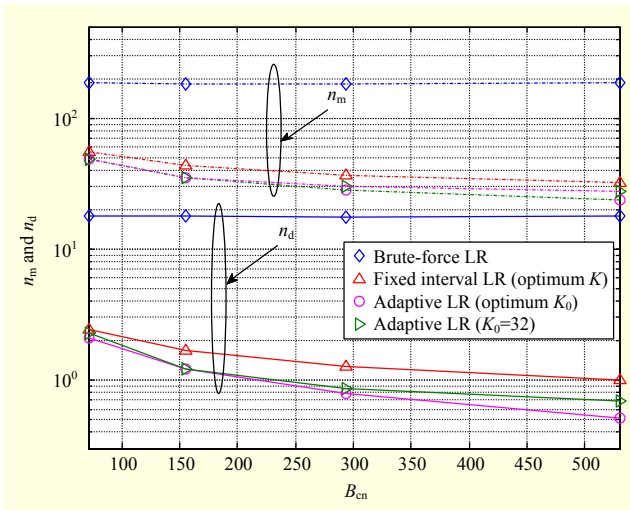


Fig. 8. Comparison of computational complexity for various LRAD schemes for 2×2 MIMO-OFDM systems.

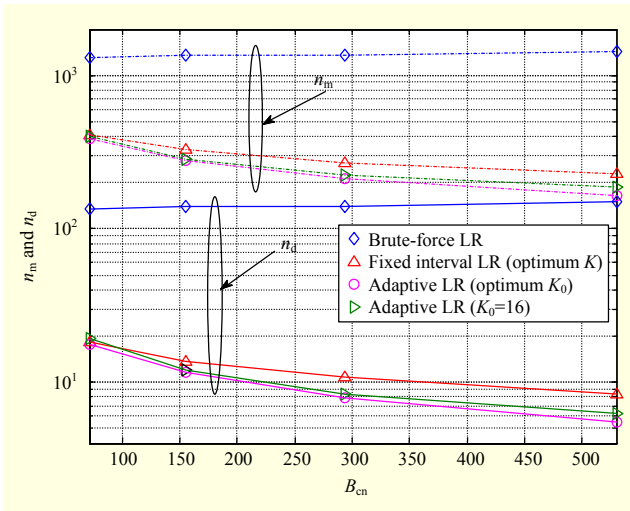


Fig. 9. Comparison of computational complexity for various LRAD schemes for 4×4 MIMO-OFDM systems.

the adaptive LR algorithm is trivial. Due to the benefits brought by the halve mode, the adaptive LR algorithm is quite immune to the spatial correlation.

Figures 8 and 9 illustrate the computational complexities in terms of n_m and n_d versus B_{cn} for various LRAD schemes. We note from the results that the adaptive algorithm with an optimum initial interval setting outperforms the other two LR schemes mentioned above with respect to computational efficiency. For example, in the 4×4 case with $B_{cn} \approx 530$, the adaptive LR algorithm requires only 11.4% ($= 164/1,434$) of the multiplications and 3.7% ($= 5.5/150$) of the divisions required by the brute-force LR algorithm and only 72.2% ($= 164/227$) of the multiplications and 65.5% ($= 5.5/8.4$) of the divisions required by the fixed interval LR algorithm.

In a real system, the mobile device may not have the channel coherence bandwidth information or does not need to measure the instantaneous coherence bandwidth all the time; therefore, it may be difficult for mobile devices to apply optimum initial intervals. For this reason, we include the simulation results for the case in which a constant value of a suboptimum initial interval, $K_0 = 32$ for 2×2 and $K_0 = 16$ for 4×4 , is applied to the adaptive LR algorithm irrespective of B_{cn} . The results reveal that even when a globally suboptimum initial interval is employed instead of the optimum initial interval, the complexity reduction performance of the adaptive LR algorithm will not degrade much and still performs significantly better than the other two algorithms. This merit comes from the adjustable initial interval setting in the halve mode of the adaptive LR scheme, which accommodates the fluctuations of channel frequency selectivity.

If we properly set the initial interval K_0 , we can roughly estimate the average computational complexity per channel matrix for the adaptive LR algorithm:

$$C_{\text{adaptive}} \approx p_B \times C_{\text{matrix mult}} + (1 - p_B) \times C_{\text{halve}} \quad (10)$$

$$\approx (1 - p_B) \times C_{\text{halve}}, \quad (11)$$

where $C_{\text{matrix mult}}$ denotes the computational complexity for one matrix multiplication in (4), and C_{halve} denotes the average computational complexity of one LR operation in step 3 and step 11 of the halve mode in Fig. 1. As $C_{\text{matrix mult}}$ is typically much smaller than C_{halve} , C_{adaptive} can be further approximated as (11). This estimate implies that we can effectively reduce the computational complexity to approximately a fraction of the computation complexity of one LR operation in the halve mode. For example, for the 2×2 case, with optimum K_0 at $B_{cn} \approx 150$, 19% ($= 35/184$) of the brute-force LR algorithm multiplications are needed, and this roughly agrees with $(1 - p_B) = 17\%$, where $p_B = 83\%$.

VI. Conclusion

In this paper, we analyzed the relationship between channel coherence bandwidth and two complexity-reduced LRAD algorithms for MIMO-OFDM systems under correlated fading channels. Computational redundancy is significantly eliminated by activating the halve mode in the adaptive LR algorithm that accommodates the fluctuation of frequency correlation. Building upon our previous work [5], we analyzed the impact of the space-frequency correlation on these two LR algorithms. Simulation results showed that the adaptive LR algorithm is more immune to the spatial correlation than the fixed interval LR algorithm. In addition, simulation demonstrated that the adaptive LR algorithm with optimum

initial interval settings effectively outperforms the conventional LR schemes in terms of computational efficiency without any performance degradation. Furthermore, the adaptive LR algorithm with a suboptimum initial interval setting achieves acceptable complexities and is sufficiently feasible in real wireless communication systems.

References

- [1] G.L. Stuber et al., "Broadband MIMO-OFDM Wireless Communications," *Proc. IEEE*, vol. 92, no. 2, Feb. 2004, pp. 271-294.
- [2] A.K. Lenstra, H.W. Lenstra, and L. Lovász, "Factoring Polynomials with Rational Coefficients," *Math. Ann.*, vol. 261, no. 4, Dec. 1982, pp. 515-534.
- [3] H. Najafi, M.E.D. Jafari, and M.O. Damen, "On Adaptive Lattice Reduction over Correlated Fading Channels," *IEEE Trans. Commun.*, vol. 59, no. 5, May 2011, pp. 1224-1227.
- [4] K. Choi et al., "Block-Mode Lattice Reduction for Low-Complexity MIMO Detection," *ETRI J.*, vol. 34, no. 1, Feb. 2012, pp. 110-113.
- [5] W. Liu, K. Choi, and H. Liu, "Computationally Efficient Lattice Reduction for MIMO-OFDM Systems," *Proc. IEEE 6th Int. Conf. Wireless Mobile Computing, Netw., Commun.*, Oct. 2010, pp. 264-267.
- [6] X. Lu, P. Silvola, and M. Juntti, "Lattice Reduction Based Detection Algorithms in High Correlated MIMO-OFDM System," *Proc. 17th Int. Symp. Personal, Indoor Mobile Radio Commun.*, Sept. 2006, pp. 1-5.
- [7] A. Murray and S. Weller, "Performance and Complexity of Adaptive Lattice Reduction in Fading Channels," *Commun. Theory Workshop, AusCTW*, Australia, Feb. 2009, pp. 17-22.
- [8] B. Choi et al., "Complexity Reduction for Lattice Reduction Aided Detection in MIMO-OFDM Systems," *Proc. 2nd Int. Conf. Computer Autom. Engineering (ICCAE)*, vol. 2, Feb. 2010, pp. 801-806.
- [9] T. Hwang et al., "OFDM and Its Wireless Applications: A Survey," *IEEE Trans. Veh. Technol.*, vol. 58, no. 4, May 2009, pp. 1673-1694.
- [10] W. Xu and S. Zekavat, "Non-Line-of-Sight Identification via Space-Frequency Correlation in MIMO-OFDM Systems: A Preliminary Study," *Proc. MILCOM*, Oct. 2010, pp. 1619-1623.
- [11] H. Karaa, R. Adve, and A. Tenenbaum, "Linear Precoding for Multiuser MIMO-OFDM Systems," *Proc. IEEE ICC*, June 2007, pp. 2797-2802.
- [12] X. Zhu and J. Xue, "On the Correlation of Subcarriers in Grouped Linear Constellation Precoding OFDM Systems Over Frequency Selective Fading," *Proc. IEEE VTC*, May 2006, pp. 1431-1435.



Wei Liu received his BS in communication engineering from North China University of Technology, Beijing, China, in 2006 and his MS from Beijing University of Posts and Telecommunications, Beijing, China, in 2009. He is currently working toward his PhD with the Department of Electrical Engineering and Computer Science in Oregon State University, Corvallis, OR, USA. His research interests include MIMO-OFDM transceiver design and signal processing techniques for multi-user communications.



Kwonhue Choi received his BS, MS, and PhD in electronic and electrical engineering from Pohang University of Science and Technology (POSTECH), Pohang, Korea, in 1994, 1996, and 2000, respectively. From 2000 to 2003, he was a member of the senior research staff at ETRI, Daejeon, Rep. of Korea, working toward the development of efficient transmission algorithms for satellite communications. He was a visiting professor at Oregon State University, Corvallis, OR, USA, from September 2008 to October 2009. He is currently with Yeungnam University, Gyongsan, Rep. of Korea, as an associate professor. His research interests include performance analysis of wireless communication systems, digital modem algorithm design, the efficient multiple access, diversity schemes for a wireless fading channel environment, cooperative communications, and complexity reduced MIMO transceiver design.



Huaping Liu received his BS and MS in electrical engineering from Nanjing University of Posts and Telecommunications, Nanjing, China, in 1987 and 1990, respectively, and his PhD in electrical engineering from the New Jersey Institute of Technology, Newark, NJ, USA, in 1997. From July 1997 to July 2001, he was with Lucent Technologies, Whippany, NJ, USA. He joined the School of Electrical Engineering and Computer Science, Oregon State University, Corvallis, OR, USA, in 2001 and has been a professor there since 2011. His research interests include ultra-wideband systems, multiple-input multiple-output antenna systems, channel coding, and modulation and detection techniques for multiuser communications. Dr. Liu served as an associate editor for the *IEEE Transactions on Vehicular Technology* and the *IEEE Communications Letters*, from 2009 to 2011. He is currently an editor for the *Journal of Communications and Networks*.